Electronic Supplementary Material (ESI) for Analyst.

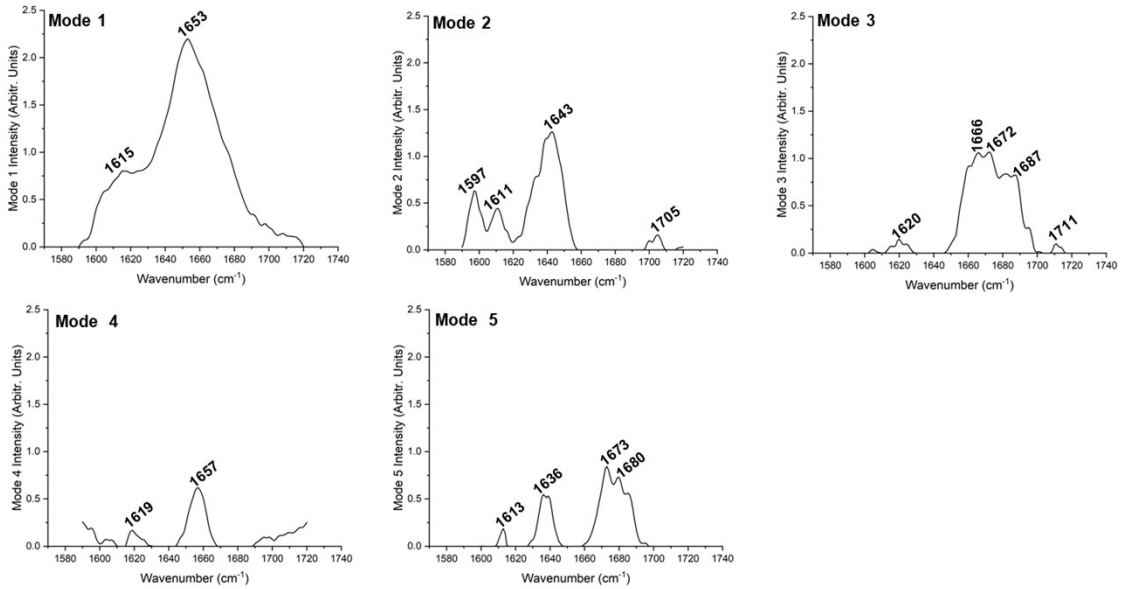

Supplementary figure 1. Non-negative matrix factorisation spectral modes from preclinical models with peaks labelled.

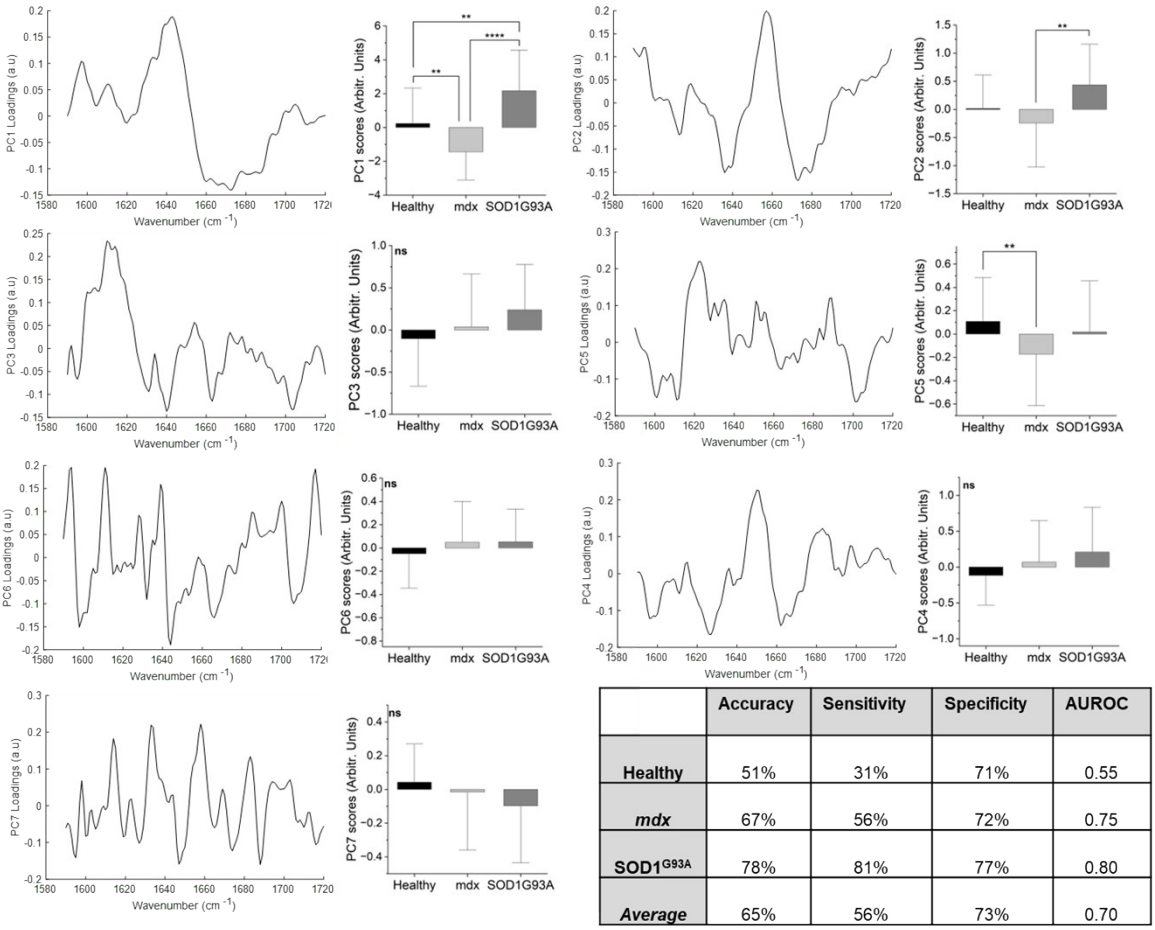

	Accuracy	Sensitivity	Specificity	AUROC
Healthy	51%	31%	71%	0.55
mdx	67%	56%	72%	0.75
SOD1^{G93A}	78%	81%	77%	0.80
Average	65%	56%	73%	0.70

Supplementary figure 2. PCA-LDA based analysis: preclinical data.

The amide I region is subjected to a more traditional PCA-LDA approach. 7 PCs were chosen, which represent 90% of the explained variance of the data. The overall performance is weaker than NMF-LDA and the positive/negative loadings are more difficult to interpret.

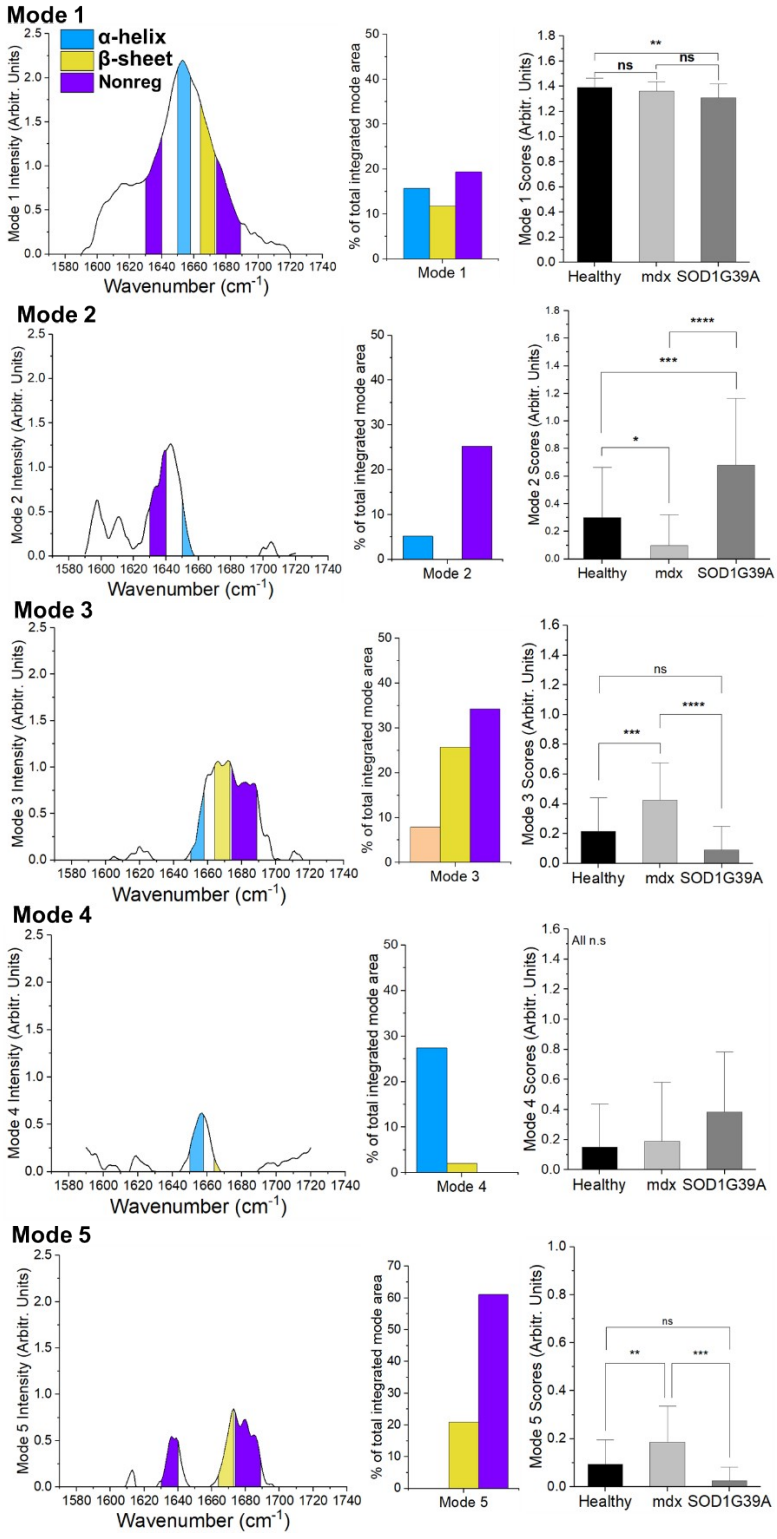

Supplementary figure 3. Assessing conformational differences in the modes with a simple integrated area approach: preclinical data.

In this analysis, the area under the peak window for different secondary structure configurations is integrated. This is a much simpler analysis than peak fitting and shows similar results that match the peak fitting analysis in the spectra (figure 1) and the modes (figure 2). This approach was kept intentionally simple, and, although the non-negative constrain often pulls the profile down to zero, we note that some area values will be affected by relative importance of adjacent wavenumbers.

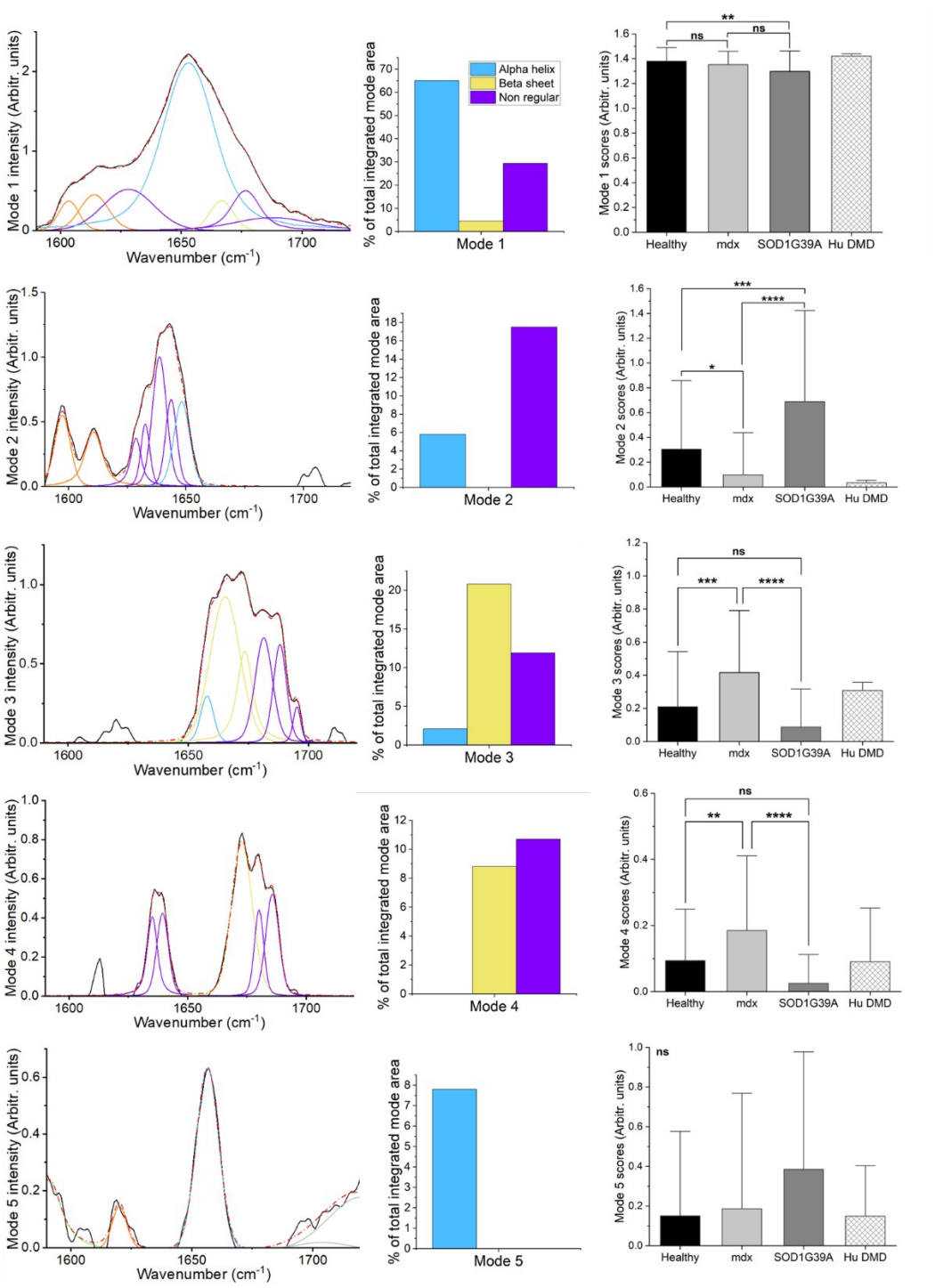

Supplemental figure 4. Non-negative matrix factorisation derived spectral patterns including human DMD samples.

In this analysis, human DMD samples (n=3) have been included in the matrix factorisation. The samples were from boys aged 2, 4, and 10 years and taken from the quadriceps muscle. The small number of samples means that the modes are essentially unchanged from the mouse-sample only analysis (figure 3), with the one exception that the order of modes 4 and 5 has been reversed. As the number of human DMD samples is small, statistical analysis have not been performed with the human data; however, the human data broadly matches the mouse data.

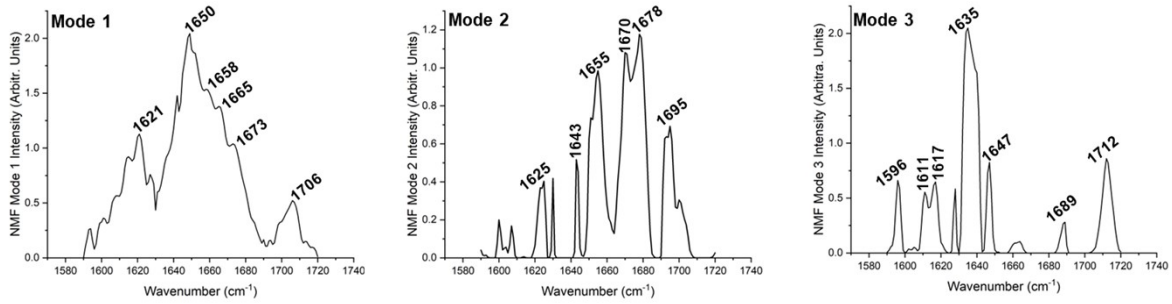

Supplemental figure 5. Non-negative matrix factorisation spectral modes from human tissue with peaks labelled.

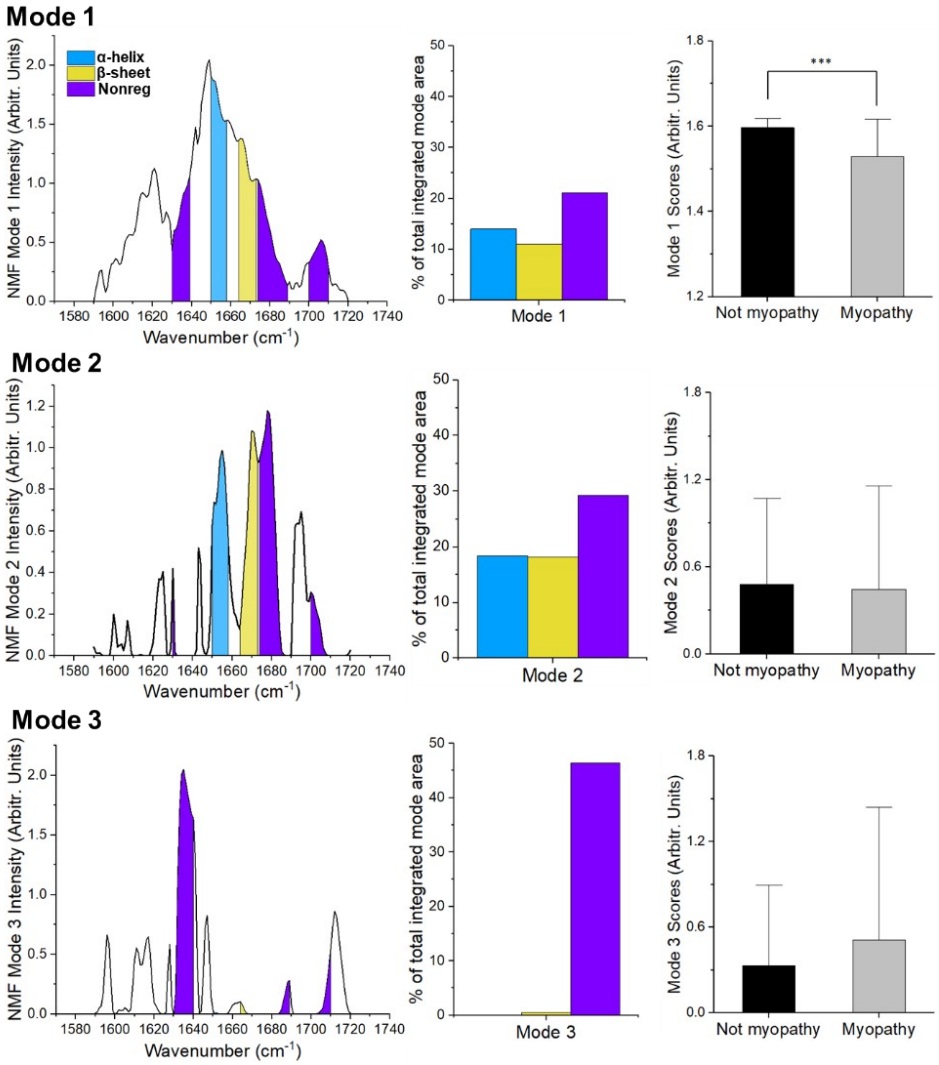

Supplemental figure 6. Assessing conformational differences in the modes with a simple integrated area approach: human data.

In this analysis, the area under the peak window for the different secondary structure configurations is integrated.

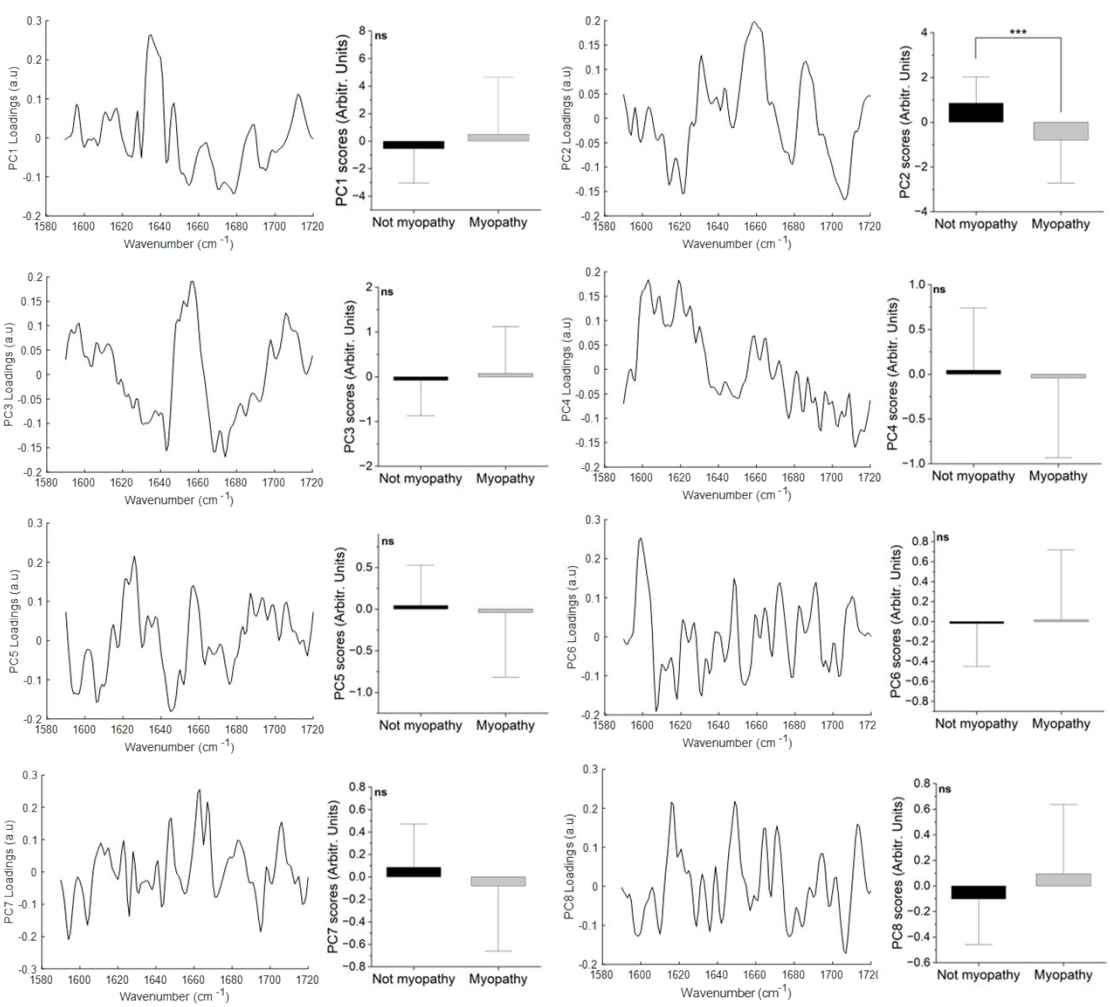

	Accuracy	Sensitivity	Specificity	AUROC
Not myopathy vs. Myopathy	67%	65%	68%	0.74

Supplemental figure 7. PCA-LDA of the amide I region: human data.

	Myopathy (n=27)	Not myopathy muscle disease (n=27)
Gender (Male: Female)	17:10	12:15
Mean Age (Range), in years	51 (22-80)	47 (23-80)
Muscle biopsied (n)		
Biceps	2	4
Quadriceps	9	5
Tibialis anterior	11	-
Deltoid	7	9
Gracilis/semitendinosus		10
Clinico-pathological diagnoses (n)		
m.3243A>G variant	11	
POLG-related mitochondrial disease	3	
single large-scale mtDNA deletion	1	
Metabolic myopathy	1	
Myopathy: unknown aetiology	5	
Dystrophic myopathy	4	
Inclusion body myositis	1	
Subacute idiopathic inflammatory myopathy	2	
Healthy volunteer		10
Vascular dementia		1
Cerebellar ataxia		8
Lumbar radiculopathy		1
Myaesthenia gravis		1
Fibromyalgia		1
Elevated CK: malignant hyperthermia		1
Elevated CK: statin-related		2
Diabatic neuropathy		1
Medical myelopathy		1
Sensory ganglionopathy		1

Supplementary table 1. Demographic and clinical characteristics of human participants.

Peak (left to right)	% area	Centre	FWHM
Healthy			
1	1.9	1601	9.5
2	9.3	1613	18.8
3	4.7	1630	23.9
4	73.3	1653	35.1
5	4.6	1673	34.2
6	6.2	1678	20.4
mdx			
1	1.9	1603	8.1
2	10.1	1614	17.7
3	9.7	1634	21.3
4	48.4	1653	24.6
5	19.3	1668	22.4
6	10.6	1681	22.3
SOD1^{G93A}			
1	2.1	1599	8.8
2	10.1	1612	18.2
3	5.6	1630	27.6
4	68	1650	29.9
5	5.6	1665	15.7
6	8.6	1677	16.1

Supplemental table 2. Peak characteristics from the preclinical peak fitting analysis.

Peak (left to right)	% area	Centre	FWHM
Not myopathy			
1	4.1	1605	20.4
2	14.6	1619	16.3
3	6.8	1637	9.2
4	41.4	1650	19.6
5	20	1665	18.9
6	7.7	1676	12
7	5.4	1705	16.3
Myopathy			
1	2.8	1597	11.1
2	20.8	1618	19.4
3	7.7	1637	8.4
4	29.5	1650	15.9
5	25.7	1667	20
6	4.0	1677	8.9
7	9.5	1705	18.3

Supplemental table 3. Peak characteristics from the human sample peak fitting analysis.